

Effects of flapping–pitching phase difference on the aerodynamic performance of hovering dragonfly wings

Haozhe Wang[1,2], Jialong Wang [1], Zhantao Li [1,2], Wenqing Yang [1,2] & Xiaojun Yang[a,1,2,3]

[1] School of Aeronautics, Northwestern Polytechnical University, Xi' an 710072, China.
[2] National Key Laboratory of Aircraft Configuration Design, Xi'an, Shaanxi, 710072, China.
[3] Research & Development Institute of Northwestern Polytechnical University in Shenzhen, Shenzhen, Guangdong, 518057, China.
[a)] Author to whom correspondence should be addressed: xjyang518@nwpu.edu.cn

Abstract

Dragonflies, as representative insects with a tandem-wing configuration, can independently control their wings through thoracic muscle actuation. Phase differences commonly exist among the three wing-motion degrees of freedom. This study focuses on the phase difference between flapping and pitching motions. A realistic dragonfly wing computational model was established, and experimentally observed hovering kinematics were applied. Five phase-difference cases ranging from 0° to 180° were investigated to evaluate the aerodynamic characteristics of tandem wings. Aerodynamic performance was analyzed using lift and thrust coefficients, flow-field structures, and power efficiency. The results show that a 45° phase difference between flapping and pitching motions generates the largest time-averaged vertical and horizontal forces. However, when aerodynamic efficiency and power consumption are comprehensively considered, a 90° phase difference is more favorable for hovering flight of dragonfly-inspired tandem wings.

Keywords: Dragonfly flight, Tandem-wing, Aerodynamics, Hovering flight

1. Introduction

Dragonflies, as representative flying insects with a typical tandem-wing configuration, can independently control their wings through thoracic muscle actuation, enabling three degrees of freedom in wing motion—flapping, pitching, and sweeping [1]. By adjusting wing kinematic parameters, favorable aerodynamic coupling and wake interactions between the forewings and hindwings can be achieved, thereby enhancing lift and thrust performance.

The multi-degree-of-freedom motion of dragonfly tandem wings involves numerous kinematic parameter combinations, and it is inferred that the phase difference between flapping and pitching motions significantly affects aerodynamic performance. K. B. Lua et al. [2] investigated the effects of forewing–hindwing phase difference and wing spacing on aerodynamic performance through both experiments and numerical simulations. Their results showed that increasing wing spacing produces an effect similar to reducing phase difference, and an approximate mathematical relationship between these two parameters was proposed. Shanmugam et al. [3] analyzed the influence of phase difference between plunging and pitching motions of a two-dimensional elliptical airfoil during hovering, finding that the maximum mean lift coefficient occurs at phase differences of 27°–60°, while the highest lift efficiency is achieved at 0°–15°. Liu et al. [4] reported that dragonflies adjust wing kinematic parameters, including phase difference, during different flight modes, leading to distinct spatial flow-field structures around the forewings and hindwings. This indicates that the aerodynamic coupling process between the two wings varies with flight condition. Guglielmini et al. [5] found that, under hovering conditions, pitching motion is the sole mechanism for thrust generation in a two-dimensional airfoil, and that the maximum propulsive efficiency is achieved when the phase difference between plunging and pitching motions is approximately 80°.

However, most previous studies on the phase difference between flapping and pitching motions have been conducted under two-dimensional conditions and generally employed identical airfoils or flat-plate tandem wings. To clarify the influence of flapping–pitching phase difference in dragonfly wings,

a three-dimensional bio-inspired dragonfly tandem-wing computational model was established. Taking the phase difference between flapping and pitching motions as the primary parameter, numerical simulations were performed to investigate the effects of phase variation among wing-motion degrees of freedom on the aerodynamic performance of tandem wings. The results of this study can provide theoretical guidance for the design of dragonfly-inspired tandem flapping-wing micro air vehicles.

2. Materials and Methods

2.1 Tandem Wings Motion model

To investigate the influence of the phase difference between flapping and pitching motions on the aerodynamic characteristics of tandem wings, a bio-inspired dragonfly tandem flapping-wing model was established based on the morphology of a real dragonfly wing (as shown in Figure 1). The main geometric parameters of the model are listed in Table 1.

Table 1 – Static parameters of the tandem wing model

Parameters	Value
Wing area of FW	$4.282\times10^{-4}m^2$
Wing area of HW	$5.183\times10^{-4}m^2$
Distance between the wing heel and the symmetry plane(d)	$8.67\times10^{-3}m$
Wing thickness(h)	$8.6\times10^{-5}m$

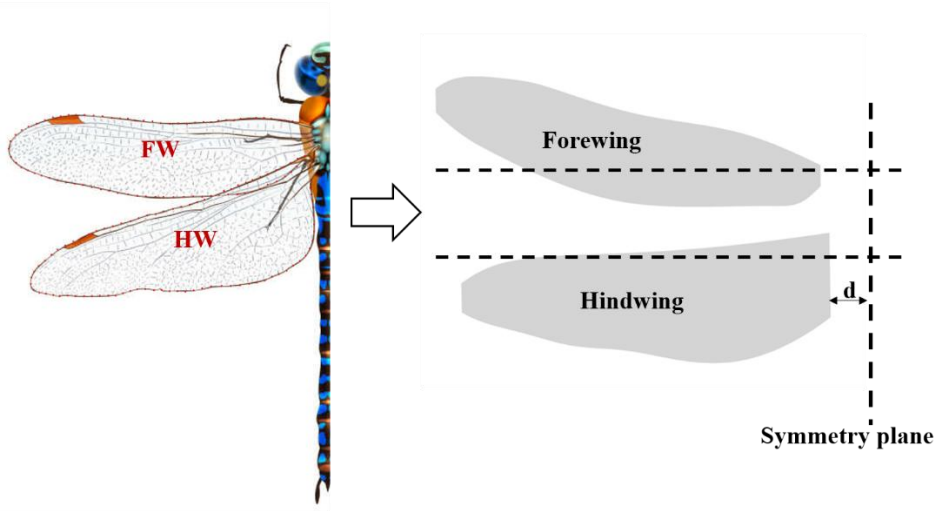


Figure 1 – Tandem wing model.

Reasonable kinematic conditions were applied to the established tandem flapping-wing model for numerical simulation. Figure 2 illustrates the rotational axes and directions of the three typical degrees of freedom in dragonfly wing motion. Here, β represents the stroke-plane angle of the tandem-wing model. The flapping motion rotates about the dragonfly body axis, the pitching motion rotates about an axis located at the quarter-chord position from the leading edge, and the sweeping motion rotates about an axis perpendicular to the wing surface at the wing root along the leading edge. The governing functions of these three degrees of freedom are expressed as follows:

$$\varphi(t) = \varphi_m \sin(2\pi ft) \tag{1}$$

$$\alpha(t) = \alpha_m \sin(2\pi ft - \psi_{pp}) \tag{2}$$

$$\gamma(t) = \gamma_m \sin(4\pi ft - \psi_{ps}) \tag{3}$$

In the above equations, $\varphi(t)$, $\alpha(t)$, and $\gamma(t)$ denote the angular displacements of the flapping, pitching, and sweeping motions, respectively. φ_m, α_m, and γ_m are the corresponding motion amplitudes. ψ_{pp} denotes the phase difference between wing flapping and pitching motions, which serves as the research variable in this paper. Five values within the range of 0°~180° are selected for investigation. ψ_{ps} represents the phase difference between wing flapping and sweeping motions. f and t denote the flapping frequency and time. The basic kinematic parameters are selected based on the detailed observations of dragonfly hovering flight reported by Zou et al. [6], as summarized in Table 2. Under hovering conditions, the phase difference between the flapping motions of the forewing and hindwing is set to 180° [7].

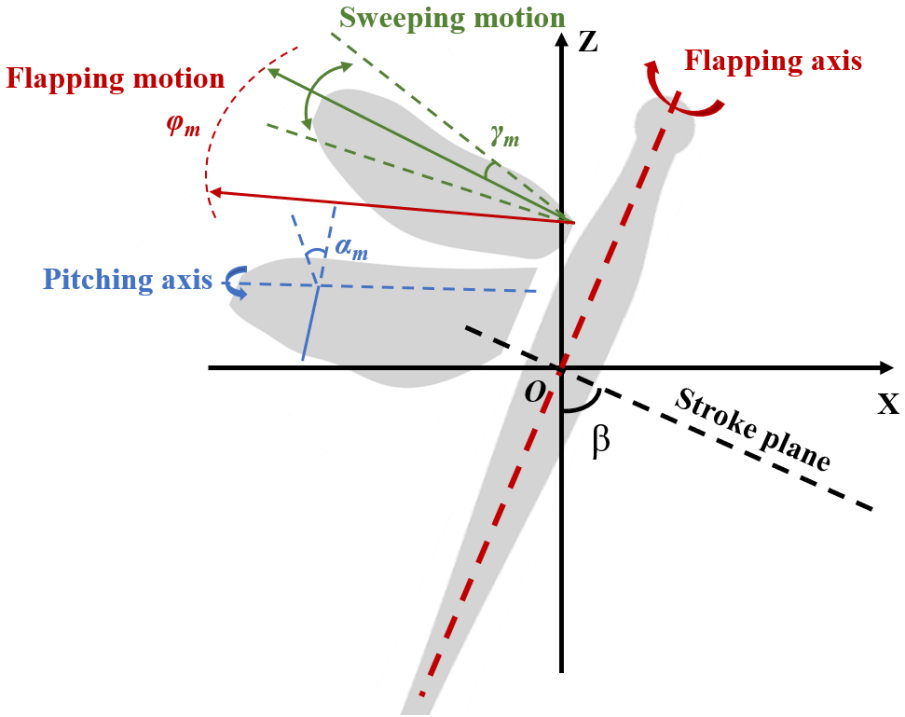


Figure 2 – Definition of the three degree of freedom wing motions of a dragonfly.

Table 2 – Computational and kinematic parameters

Parameters	Value
Re	1286
Computational model	Laminar
Frequency (f)	33.1Hz
β	FW:82.9°, HW:82.5°
φ_m	FW:28.4°, HW:35.5°
α_m	FW:57.7°, HW:54.4°
γ_m	FW:4.1°, HW:4.2°
ψ_{pp}	0°,45°,90°,135°,180°
ψ_{ps}	15°

The forces obtained from the calculation results are divided into vertical force F_V and horizontal force F_H. In Figure 2, the vertical force is along the Z-axis direction and the horizontal force is along the X-axis direction. The calculation formula for the time-averaged force coefficient is shown below.

$$\overline{C_V} = \frac{1}{T}\int_t^{t+T} \frac{F_V}{\frac{1}{2}\rho u^2 S} dt \quad (4)$$

$$\overline{C_H} = \frac{1}{T}\int_t^{t+T} \frac{F_H}{\frac{1}{2}\rho u^2 S} dt \quad (5)$$

Where T is the time taken for one cycle of movement.

2.2 Computational conditions

In this study, transient numerical simulations were conducted using computational fluid dynamics (CFD) software by solving the transient incompressible continuity equation and the Navier–Stokes equations. All cases were simulated using a laminar flow model. Momentum, turbulent kinematic energy, and specific dissipation rate are discretized with a second-order upwind scheme. Second-order accuracy is applied to calculate the pressure. Transient Formulation is First Order Implicit. A coupled algorithm is employed for the pressure-velocity coupling.

To focus the present study on the effects of kinematic parameters on tandem wing aerodynamics, the influence of the fuselage is neglected in the CFD analysis. Accordingly, only the wing geometries are modeled, meshed, and analyzed. The computational domain and wing surface mesh are shown in Figure 3. Figure 3(a) presents the stationary background mesh. Under hovering conditions, no freestream velocity is prescribed, and the computational domain is defined with one symmetry plane and five pressure outlets as boundary conditions. Figure 3(b) shows the dynamic component mesh, where the unstructured overset mesh moves rigidly together with the wings. Figure 3(c) illustrates the structured surface mesh on the wings. The height of the first boundary-layer cell is set to 0.08 mm.

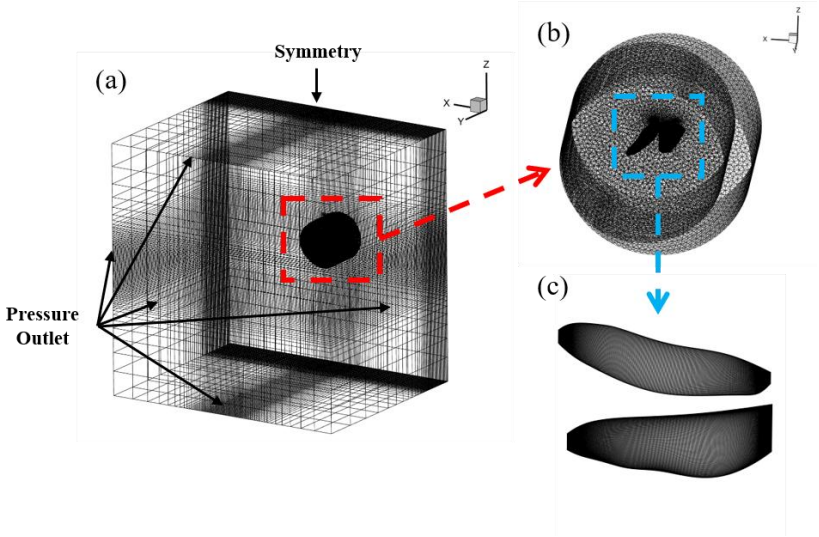


Figure 3 – Computational mesh of the dragonfly tandem wings.

2.3 Solver validation

The water-tunnel experiments conducted by S. Heathcote et al. [8] in 2006 were selected to validate the numerical solver used in this study. A three-dimensional half-span rectangular wing with a NACA0012 airfoil was placed in a water tunnel and driven by a mechanical actuator to perform a sinusoidal heaving motion perpendicular to the freestream. The half-span of the wing was 300 mm, corresponding to an equivalent full-wing aspect ratio of 6. A three-dimensional CFD model was established according to the experimental configuration and geometric dimensions, and the prescribed heaving motion was imposed through the corresponding motion function to perform numerical simulations for validation against the reference experiment. The thrust coefficient obtained from the numerical simulation was compared with the experimental measurements reported by Heathcote et al., as shown in Figure 4. The results demonstrate good agreement in both the overall trend and numerical values, with only slight deviations near the peak and trough regions. These

discrepancies may be attributed to minor airfoil deformation during the physical experiment. The comparison confirms that the overset-grid method adopted in this study can effectively predict the lift and thrust characteristics of such unsteady aerodynamic problems.

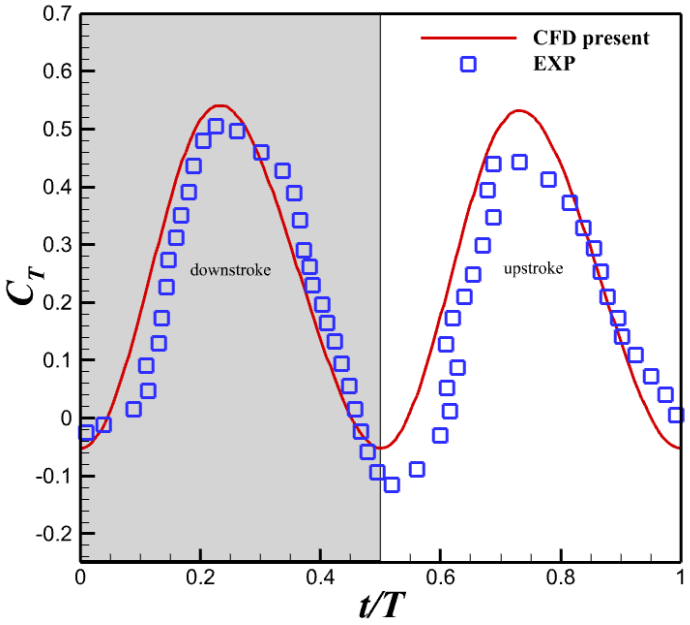


Figure 4 – Comparison of experiment and CFD simulations.

3. Results

3.1 Force coefficient analysis

To investigate the influence of the phase difference between flapping and pitching motions on the hovering aerodynamic performance of tandem wings, five cases with different flapping–pitching phase differences were simulated. Each case was computed for three flapping cycles, and only the results from the final cycle were analyzed.

Figure 5 presents the variations in vertical-force and horizontal-force coefficients of the tandem wings. In the instantaneous force-coefficient curves shown in Figure 5(a) and Figure 5(c), different colors represent different flapping–pitching phase differences, as indicated in the legends. It can be observed that when the phase difference is 0°, both the instantaneous vertical-force and horizontal-force coefficients exhibit the largest fluctuation amplitudes. In contrast, the 90° and 135° cases show the smallest fluctuation ranges, while for the 180° case, the instantaneous vertical-force coefficient remains below zero for most of the cycle.

Further examination of the time-averaged force coefficients in Figure 5(b) and Figure 5(d) shows that, with increasing phase difference between flapping and pitching motions, both the time-averaged vertical-force and horizontal-force coefficients first increase and then decrease. The maximum time-averaged force coefficients are achieved at a phase difference of 45°. It is also noteworthy that the time-averaged vertical-force coefficient is approximately one order of magnitude larger than the horizontal-force coefficient, which is consistent with the hovering flight condition considered in this study.

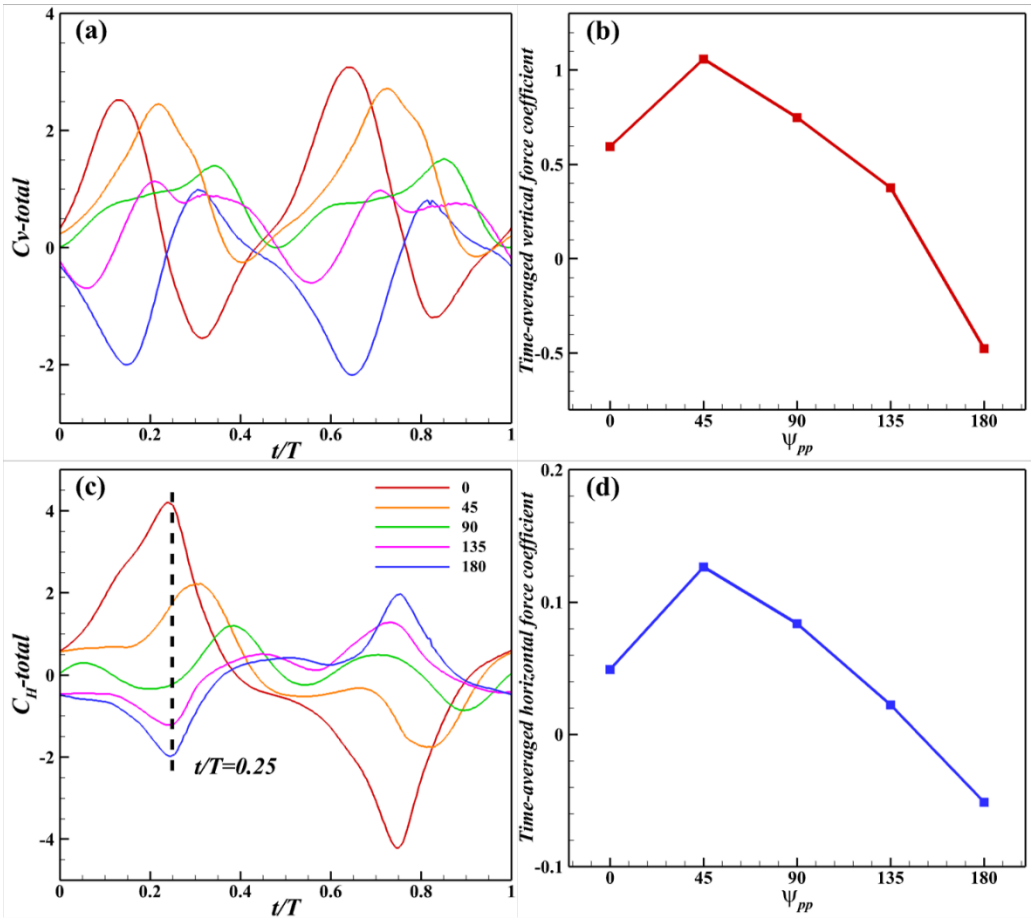


Figure 5 – Force coefficients of tandem wings with different flapping pitching phase differences.(a) Instantaneous vertical force coefficient; (b) Time-averaged vertical force coefficient; (c) Instantaneous horizontal force coefficient; (d) Time-averaged horizontal force coefficient.

To further investigate the individual contributions of the forewing and hindwing in the tandem configuration, Figure 6 presents the instantaneous vertical and horizontal force coefficient for each wing. In the figure, the grey shaded region denotes the downstroke phase, while the white background indicates the upstroke phase. As shown in Figure 6(a), the forewing exhibits two peaks in the vertical force coefficient under all flapping–pitching phase differences, with the first peak being more pronounced. A closer examination of the first peak reveals that its occurrence is progressively delayed as the phase difference increases. A similar trend is also observed for the hindwing in Figure 6(b). In addition, the peak magnitude of the hindwing vertical force coefficient continuously decreases with increasing phase difference. When the phase difference reaches 180°, the peak becomes nearly indistinguishable and approaches a flat response.

Figure 6(c) and (d) present the instantaneous horizontal force coefficients of the forewing and hindwing, respectively. Due to the 180° phase shift between the two wings, the timing of their peak and valley values occurs in opposite phases. Interestingly, for the forewing, the amplitude of the horizontal force coefficient increases with increasing phase difference, whereas for the hindwing, the opposite trend is observed, with the amplitude decreasing as the phase difference increases.

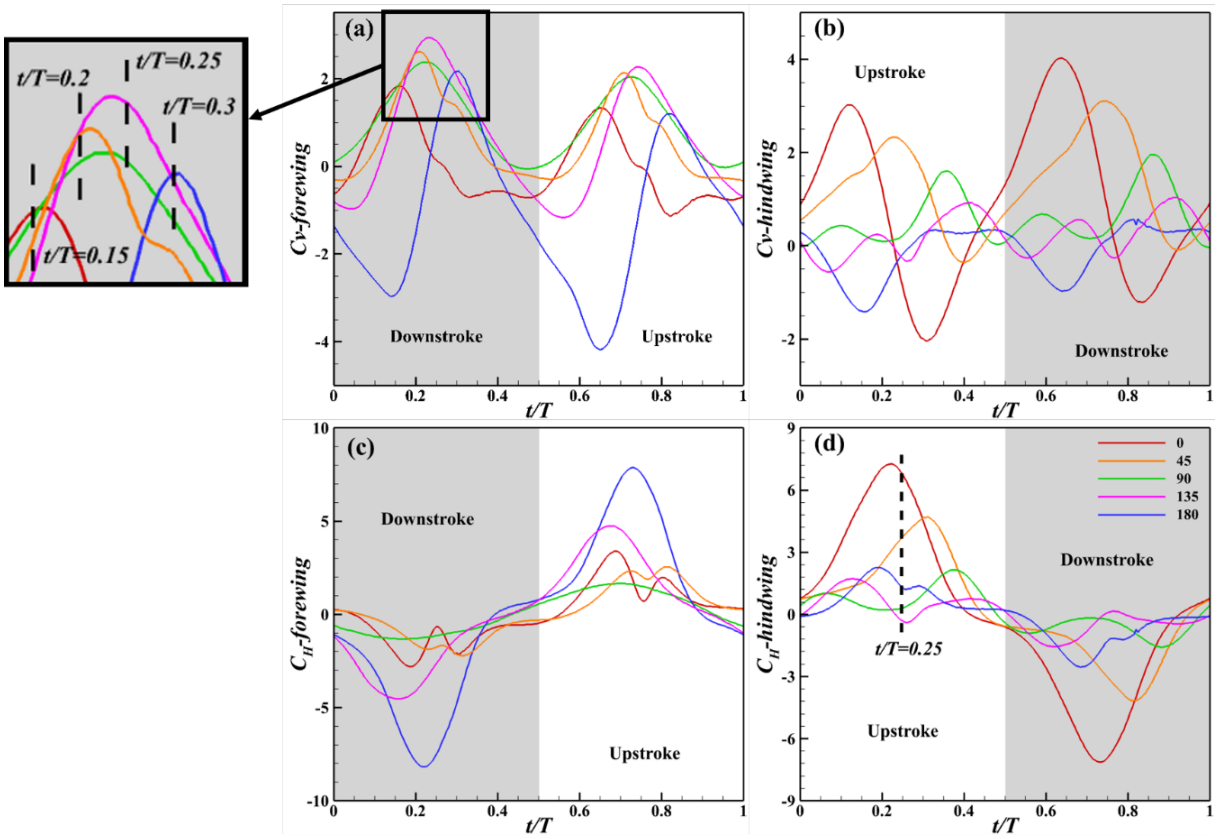


Figure 6 – Instantaneous force coefficients under different flapping pitch phase differences. (a) Vertical force coefficient of forewing; (b) Vertical force coefficient of hindwing; (c) Horizontal force coefficient of forewing; (d) Horizontal force coefficient of hindwing.

3.2 Fluid structures analysis

Based on the first peak of the forewing vertical force coefficient shown in Figure 6(a), the surface pressure coefficient distributions of the forewing at the corresponding peak instants under different flapping–pitching phase differences are extracted and analyzed, as illustrated in Figure 7. The pressure coefficient (cp) is defined by Equation (6), where u denotes the reference velocity, taken as the mean velocity of the wingtip over one flapping cycle (3.04 m/s).

$$cp = \frac{pressure}{\frac{1}{2}\rho u^2} \tag{6}$$

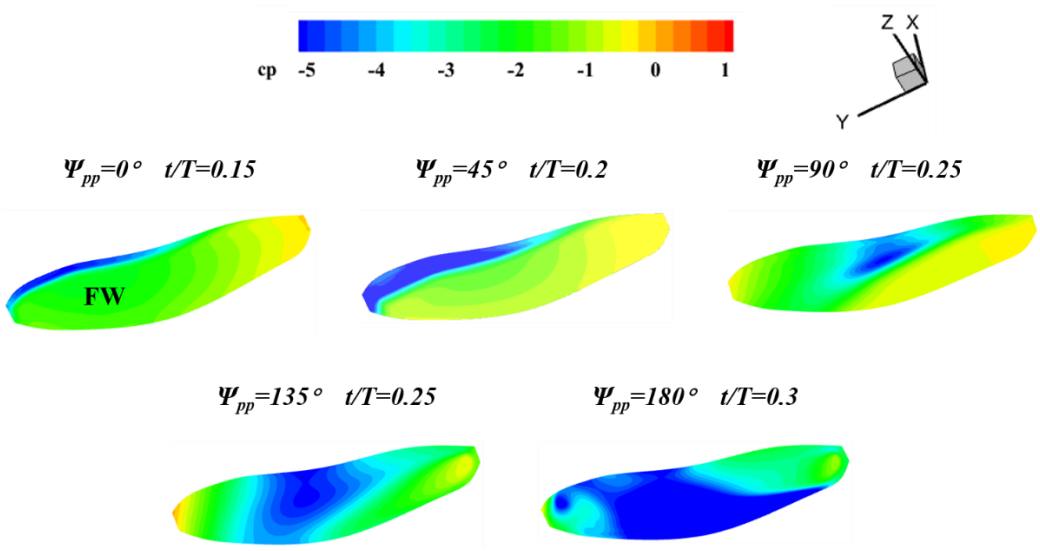


Figure 7 – Wing surface pressure coefficient with different phase difference and different time.

As illustrated in Figure 7, the distribution of the low-pressure region on the upper surface of the forewing at the peak vertical force coefficient varies with the flapping-pitching phase difference. When the phase difference is relatively small (ψ_{pp} = 0° and 45°), the suction region is primarily concentrated within a localized zone near the leading-edge wingtip. Notably, the area of the leading-edge low-pressure zone at ψ_{pp} = 45° is more than double that at ψ_{pp} = 0°. This phenomenon is directly reflected in the peak vertical force coefficients, where the peak value for ψ_{pp} = 45° exhibits an increase of nearly 40% compared to that for ψ_{pp} = 0°.

Concurrently, as the phase difference increases to 90°, the low-pressure region shifts from the wingtip to the mid-span, and migrates from the leading edge toward the mid-chord region. With a further increase in the phase difference to 135°, the low-pressure zone expands extensively, centering around the mid-span leading edge and spreading across the entire chord to the trailing edge, which corresponds to the maximum peak vertical force coefficient of the forewing. Finally, at ψ_{pp} = 180°, the occurrence of the peak value is delayed to t/T = 0.3. Interestingly, although the coverage of the low-pressure region on the upper surface reaches its maximum at this phase difference, the magnitude of the peak vertical force coefficient is not particularly pronounced. It is conjectured that this discrepancy arises because the extensive shift of the low-pressure region toward the trailing edge alters the orientation of the surface pressure resultant, thereby reducing its effective component along the vertical force direction upon decomposition.

To further analyze the horizontal force performance, the individual horizontal force coefficients (C_h) of the forewing and hindwing are examined, as shown in Figure 6(c) and (d), respectively. It is observed that the forewing C_h reaches its minimum (trough value) at t/T = 0.25, precisely when the hindwing C_h attains its peak. Conversely, an opposite trend is manifested at t/T = 0.75. Concurrently, inspection of the total horizontal force coefficient of the tandem wing system in Figure 5(c) reveals a distinct peak at t/T = 0.25. Therefore, spanwise slices of the Y-vorticity fields for both the forewing and hindwing were extracted at t/T=0.25 to elucidate the underlying aerodynamic mechanisms.

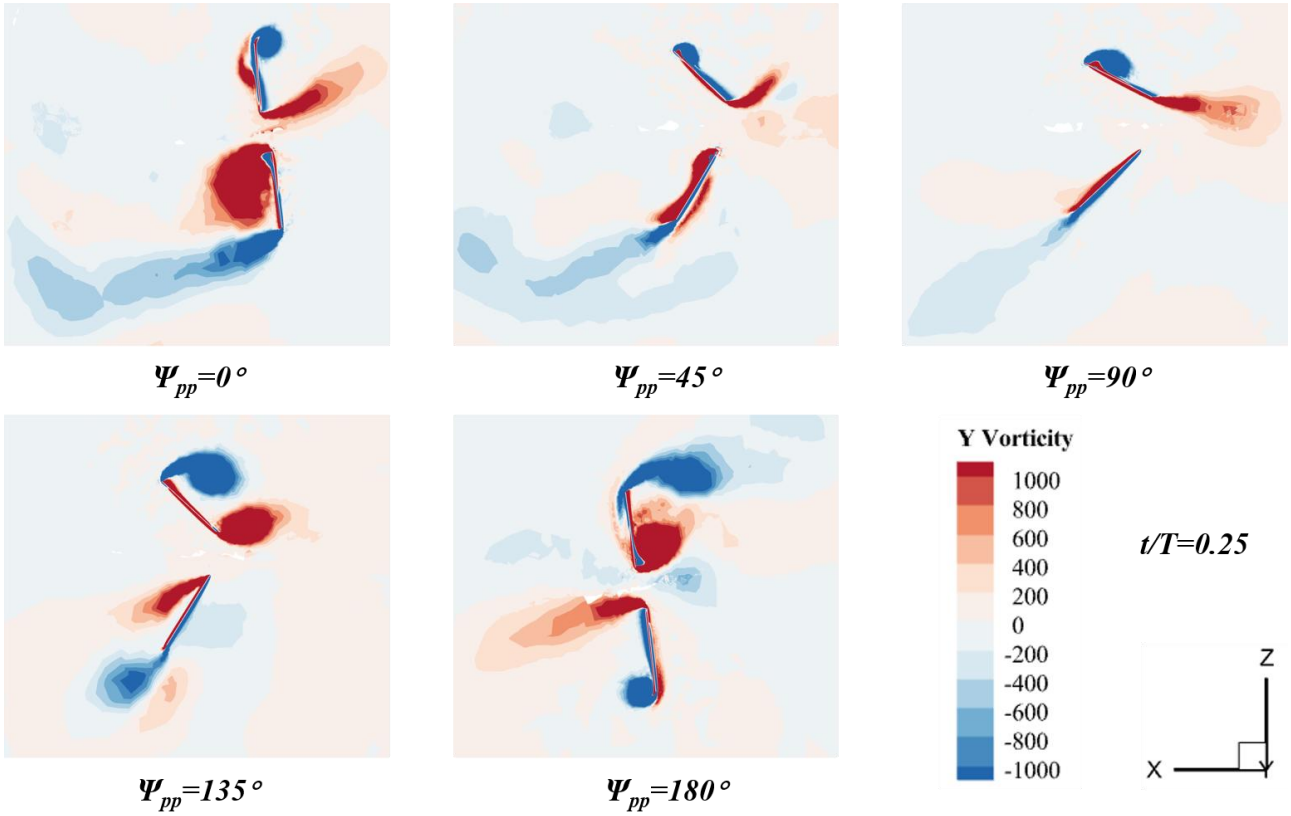


Figure 8 – Y vorticity slice of forewing and handwing.

At t/T=0.25, the forewing is in the downstroke phase while the hindwing is in the upstroke phase, resulting in opposite wing motions. As a consequence, as shown in Figure 8, the vortex shedding directions of the two wings are reversed: the forewing sheds vortices toward the negative X-direction, whereas the hindwing sheds vortices toward the positive X-direction. This opposite vortex shedding behavior explains why the forewing exhibits a negative horizontal force coefficient while the hindwing shows a positive value in Figure 6(c) and (d) at this instant.

Furthermore, examining the trailing-edge vortex (TEV) wake of the hindwing under different flapping–pitching phase differences reveals that, at relatively small phase differences (less than 90°), the TEV wake is significantly extended downstream. As the phase difference increases, the TEV becomes more attached to the wing surface with reduced wake diffusion. This behavior accounts for the reduction in the hindwing horizontal force coefficient peak observed in Figure 6(d) with increasing phase difference. Additionally, as shown in Figure 5(c), when the flapping–pitching phase difference is 0°, the peak thrust coefficient of the tandem wings is significantly higher than in other cases. This may be attributed to the reduced spacing between the forewing trailing edge and the hindwing leading edge at this instant, where the interaction between the forewing trailing-edge vortex and the hindwing leading edge forms a narrow-channel effect [9], substantially enhancing the horizontal force generation.

3.3 Power efficiency analysis

The power P, power loading PL, and propulsive efficiency η of the tandem wings are defined as follows [10]. These three performance metrics are studied for the five cases with different flapping–pitching phase differences.

$$P = -(M_x\omega_x + M_y\omega_y + M_z\omega_z) \tag{7}$$

$$C_{P_{mean}} = \frac{1}{T}\int_t^{t+T} \frac{P}{\frac{1}{2}\rho u^3 S} dt \tag{8}$$

$$PL = \frac{\overline{C_V}}{C_{P_{mean}}} \tag{9}$$

$$\eta = \frac{\overline{C_H}}{C_{P_{mean}}} \tag{10}$$

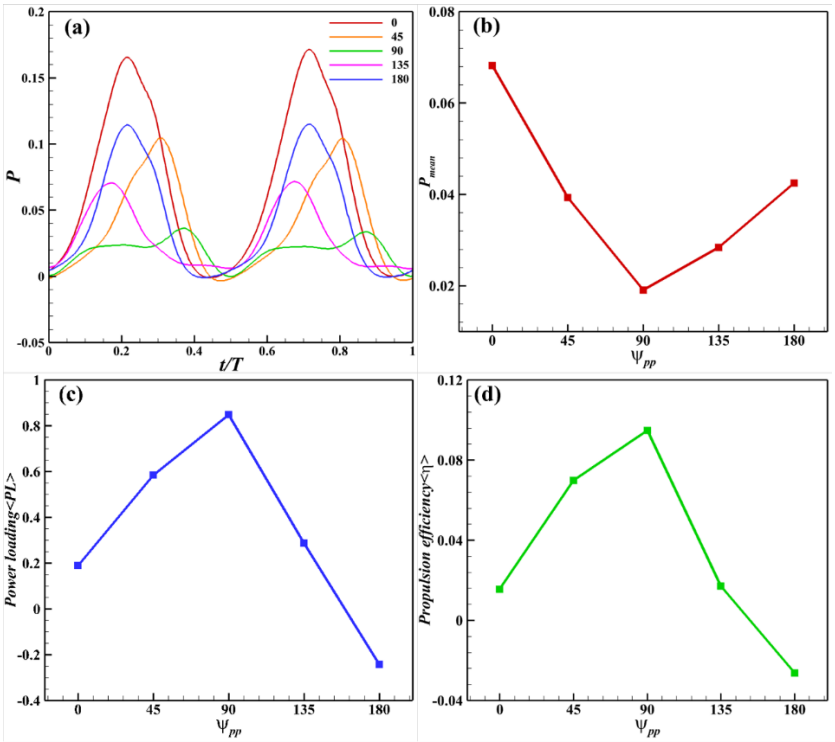


Figure 9 – Power index under different flapping and pitching phase differences. (a) Instantaneous power value; (b) Time-averaged power value; (c) Power loading; (d) Propulsion efficiency.

From the instantaneous power variation shown in Figure 9(a), it can be observed that the power consumption of the tandem wings exhibits two primary peaks within one flapping cycle. In particular, the case with a 0° flapping–pitching phase difference corresponds to the highest power consumption among all configurations. As shown in Figure 9(b), the time-averaged power first decreases and then increases with increasing phase difference, reaching a minimum at a phase difference of 90°. Figure 9(c) and (d) further indicate that both power loading (PL) and propulsive efficiency (η) achieve their maximum values at a 90° phase difference, suggesting that the tandem-wing system performs more efficiently under this condition.

4. Conclusions

In this study, an overset-grid method was employed to perform numerical simulations of a tandem-wing model with different flapping–pitching phase differences. The vertical and horizontal force coefficients of the forewing and hindwing, as well as the flow-field structures and power efficiency, were analyzed to investigate the influence of phase difference on the aerodynamic performance of tandem wings. The main conclusions are summarized as follows:

During hovering flight of tandem wings, at the peak instant of the forewing vertical force, a low-pressure region forming near the leading edge on the upper surface of the forewing plays a key role in enhancing the vertical force peak. When the phase difference is relatively small (less than 90°), this low-pressure region tends to concentrate near the leading edge, which is more favorable for vertical force augmentation. For the horizontal force coefficient, variations in the flapping–pitching phase difference alter the relative positioning between the forewing and hindwing. At peak instants, a smaller phase difference leads to a more pronounced hindwing wake, which significantly enhances horizontal force generation.

Overall, in terms of time-averaged force, a 45° phase difference yields the highest vertical and horizontal force coefficients. However, when aerodynamic efficiency is also considered, a 90° flapping–pitching phase difference is found to be more suitable for hovering flight conditions.

5. Contact Author Email Address

The contact author email address: xjyang518@nwpu.edu.cn

6. Acknowledgments

This work is financially supported by National Natural Science Foundation of China under Grants No. 52575346, and Guangdong Basic and Applied Basic Research Foundation under Grant No. 2026A1515012362.

7. Copyright Statement

The authors confirm that they, and/or their company or organization, hold copyright on all of the original material included in this paper. The authors also confirm that they have obtained permission, from the copyright holder of any third party material included in this paper, to publish it as part of their paper. The authors confirm that they give permission, or have obtained permission from the copyright holder of this paper, for the publication and distribution of this paper as part of the ICAS proceedings or as individual off-prints from the proceedings.

References

[1] Lang, Xinyu, Bifeng Song, and Wenqing Yang. "Numerical simulation of pitching motion effects on the aerodynamic performance of dragonfly-like flapping wing." *ICAS*. 2021.

[2] Lua, Kim Boon, et al. "Aerodynamics of two-dimensional flapping wings in tandem configuration." *Physics of Fluids* 28.12 (2016).

[3] Shanmugam, A. R., and C. H. Sohn. "Systematic investigation of a flapping wing in inclined stroke-plane hovering." *Journal of the Brazilian Society of Mechanical Sciences and Engineering* 41.8 (2019): 347.

[4] Liu, Xiaohui, et al. "The importance of flapping kinematic parameters in the facilitation of the different flight modes of dragonflies." *Journal of Bionic Engineering* 18.2 (2021): 419-427.

[5] Guglielmini, Laura, and Paolo Blondeaux. "Propulsive efficiency of oscillating foils." *European Journal of Mechanics-B/Fluids* 23.2 (2004): 255-278.

[6] Zou, Pei-Yi, Yu-Hsiang Lai, and Jing-Tang Yang. "Effects of phase lag on the hovering flight of damselfly and dragonfly." *Physical Review E* 100.6 (2019): 063102.

[7] Huang, Hua, and Mao Sun. "Dragonfly forewing-hindwing interaction at various flight speeds and wing phasing." *AIAA journal* 45.2 (2007): 508-511.

[8] Heathcote S, Wang Z, Gursul I. Effect of spanwise flexibility on flapping wing propulsion[J]. *Journal of fluids and structures*, 2008, 24(2): 183-199.

[9] Chang, Min, et al. "Aerodynamic Performance of Three Flapping Wings with Unequal Spacing in Tandem Formation: M. Chang et al." *Journal of Bionic Engineering* 21.4 (2024): 1662-1676.

[10] Zhu, Zhichao, et al. "Three-dimensional sweeping motion effects on hovering dragonflies." *Aerospace Science and Technology* 127 (2022): 107701.